First-principles study of structural, elastic, electronic, lattice dynamic and optical properties of *X*N (*X*=Ga, Al and B) compounds under pressure

2011 Phys. Scr. 83 065702

(http://iopscience.iop.org/1402-4896/83/6/065702)

Phys. Scr. **83** (2011) 065702 (9pp) doi:10.1088/0031-8949/83/06/065702

First-principles study of structural, elastic, electronic, lattice dynamic and optical properties of XN (X = Ga, Al and B) compounds under pressure

M Fatmi[1], B Ghebouli[2], M A Ghebouli[3] and Z K Hieba[4]

[1] Research Unit on Emerging Materials, University Ferhat Abbas of Setif, 19000, Algeria
[2] Department of Physics, University Ferhat Abbas of Setif, 19000, Algeria
[3] Department of Physics, Universitary Center of Bordj Bou-Arreridj, 34000, Algeria
[4] Department of Physics, Faculty of Science, Taif University, Ta'if, Saudi Arabia

E-mail: fatmimessaoud@yahoo.fr

Received 22 May 2010
Accepted for publication 11 April 2011
Published 12 May 2011
Online at stacks.iop.org/PhysScr/83/065702

Abstract
We have applied the pseudo-potential plane wave method to study the structural, elastic, electronic, lattice dynamic and optical properties of GaN and AlN in the wurtzite lattice and BN with zinc-blende structure. We have found that all elastic constants depend strongly on hydrostatic pressure, except for C_{44} in wurtzite AlN and GaN that shows a weaker dependence. AlN and GaN present a direct band gap Γ–Γ, whereas BN has an indirect band gap Γ–X. The indirect Γ–K band gap in AlN occurs at about 35 GPa. The top of the valence bands reflects the p electronic character for all structures. There is a gap between optical and acoustic modes only for wurtzite phases AlN and GaN. All peaks in the imaginary part of the dielectric function for the wurtzite lattice GaN and AlN move towards lower energies, while those in the zinc-blende BN structure shift towards higher energies with increasing pressure. The decrease of the static dielectric constant and static refractive index in zinc-blende BN is weaker and it can be explained by its higher elastic constants.

PACS numbers: 78.20.Ci, 71.20.Nr

(Some figures in this article are in colour only in the electronic version.)

1. Introduction

The group-III nitride semiconductors have attracted much attention because of their promising technological applications [1]. This series of materials is used in the fabrication of optoelectronic devices such as light-emitting diodes (LEDs), laser diodes and optical detectors operating in green and blue spectral regions [2, 3]. The class of group III nitrides has a high melting point, a high thermal conductivity and a large bulk modulus [4]. These properties and the wide band gaps are closely related to strong ionic and covalent bonding.

BN crystallizes normally in a hexagonal graphite-like phase; however, it can be synthesized also in zinc-blende and wurtzite structures. The cubic BN does not dissolve in iron or steel and is therefore an excellent material for the protective coating of heavy-duty tools (see [5] and references cited therein). AlN is one of the most promising materials for optoelectronic devices operating under extreme conditions. It is characterized by very short strong bonds, high ionicity, high melting point, high thermal conductivity and a large bulk modulus. In the bulk form, AlN stabilizes in the wurtzite structure; however, it has been reported that AlN can be grown in zinc-blende phase [6, 7]. GaN is a wide-gap semiconductor

that usually crystallizes in the wurtzite lattice. However, under certain conditions, zinc-blende GaN can be grown on a zinc-blende substrate. Compared to the hexagonal GaN, the metastable cubic phase has several advantages for device applications, including easy cleavage, smaller band gap and higher carrier mobility [8]. GaN is a good candidate for optoelectronic devices operating under special circumstances because of its high hardness, low compressibility, high ionicity and high thermal conductivity [8]. In this paper, we will contribute to the investigation of the AlN and GaN wurtzite lattice and BN zinc-blende structure by performing a first-principles study of some of the properties.

The remainder of this paper is divided into three parts. In section 2, we briefly describe the computational techniques used in this study. The most relevant results obtained for the structural, elastic, electronic, lattice dynamic and optical properties of these binary compounds are presented and discussed in section 3. Finally, in section 4, we summarize the main conclusions of this work.

2. Computational method

We optimized the lattice constant, internal parameter and calculated the ground state structure by using the standard CASTEP code [9], which is a plane wave pseudo-potential total energy calculation method based on density functional theory (DFT) [10]. The plane wave energy cutoff and the Brillouin zone sampling were fixed at 400 eV and $9 \times 9 \times 2$ special k-point meshes for the wurtzite lattice and $8 \times 8 \times 8$ for the zinc-blende structure. Interactions of electrons with ion cores were represented by the Vanderbilit-type ultrasoft pseudo-potential [11]. The exchange correlation potential was calculated within the generalized gradient approximation of Perdew, Burke and Ernzerhof (PBE-GGA) [12]. The states Al: $3s^2\ 3p^1$, Ga: $3d^{10}\ 4s^2\ 4p^1$, B: $2s^2\ 2p^1$ and N: $2s^2\ 2p^3$ were treated as valence states. The calculation of the optical properties requires a dense mesh of uniformly distributed k-points, where the integration was performed using a $20 \times 20 \times 20$ grid of Monkhorst-pack points.

3. Results and discussions

3.1. Structural properties

We have investigated the structural parameters of AlN and GaN in the wurtzite lattice and BN with zinc-blende structure. For the wurtzite phase, there are four atoms per hexagonal unit cell, where Ga and Al occupy the sites (0, 0, 0), (1/3, 2/3, 1/2) and the atomic positions N are (0, 0, u), (1/3, 2/3, $u + 1/2$), where u is the dimensionless internal parameter that represents the distance between the Ga and Al plane and its nearest-neighbor N plane, in units of c. For the zinc-blende BN, the atomic positions are B (0, 0, 0) and N (1/4, 1/4, 1/4). To determine the equilibrium geometry of the wurtzite phase, we optimize the volume of the unit cell V, c/a and u. The equilibrium lattice constants and internal parameters were determined by fitting the obtained total energy as a function of the atomic volume using the Birch–Murnaghan equation of state. The calculated equilibrium structural parameters for the wurtzite AlN and GaN and zinc-blende BN, along with the available experimental data [13, 14] and other calculations [15], are reported in table 1. A plot of the internal parameter of AlN and GaN is shown in figure 1. The internal parameter decreases monotonically with increasing pressure in the case of GaN, but increases in the case of AlN. The obtained B_0 and B' values from Birch–Murnaghan equation of state (EOS) fitting are listed in table 1. The bulk modulus is a measure of the crystal rigidity; thus a large compressibility corresponds to a high crystal rigidity.

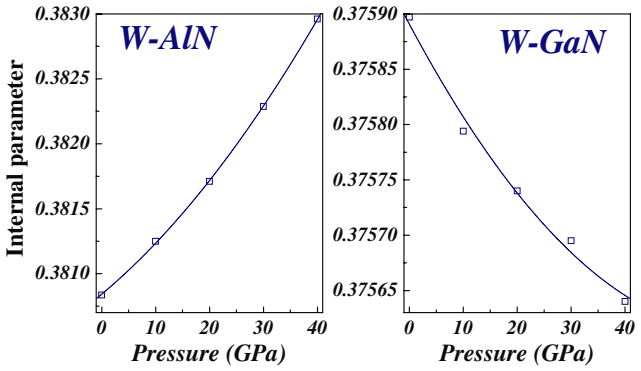

Figure 1. Internal parameters of the wurtzite lattice AlN and GaN as a function of pressure.

3.2. Elastic properties

The technique used to determine the elastic constants usually involves either the stress or the strain to a finite value. In this approach, the ground state structure is strained according to symmetry-dependent strain patterns with varying amplitude and a subsequent computing of the stress tensor after a geometry optimization with fixed cell parameters. The computed elastic constants of AlN and GaN in the wurtzite lattice and BN with zinc-blende structure at equilibrium, along with the available experimental data [16] and other calculations [17, 18], are presented in table 1. The calculated bulk modulus value obtained from elastic constants is nearly the same as that obtained from the EOS fitting. This may be an estimate of the reliability and accuracy of our calculated elastic constants. In figure 2, we present the pressure dependence of the elastic constants obtained for BN zinc-blende and wurtzite GaN and AlN using GGA in the range of hydrostatic pressures 0–40 GPa. One can see that all elastic constants show considerable increase with pressure, while C_{44} exhibits much weaker dependence on pressure in GaN and AlN. Our results for GaN and AlN wurtzite structure are in good agreement with those reported by Lepkowski *et al* [19] and show a similar variation under pressure.

We define the ductility index, μ_D, due to Pugh [20], given by $\mu_D = B/G$, and the machinability index, μ_M, due to Sun *et al* [21], given by $\mu_M = B/C_{44}$. These two indices show that a high tensile strength combined with a low shear resistance leads to good machinability. The two indices give measures of these ratios, with one index using C_{44} as the measure of shear resistance, while the other index uses the shear modulus G. The μ_D and μ_M values are listed in table 1. The obtained B/G ratio is lower than 1.75 for all these binary compounds. According to these values, AlN, GaN and BN behave as brittle material. Using the calculated elastic constants, we calculated

Table 1. Calculated structural parameters, elastic constants, shear modulus, B/G and B/C_{44} ratios, Young's modulus and Poisson's ratio of the zinc-blende BN and wurtzite AlN and GaN at zero pressure.

	Zb-BN			W-AlN			W-GaN		
	TW	Exp	Other	TW	Exp	Other	TW	Exp	Other
a_0 (Å)	3.59	3.615[a]	3.575[c]	3.062	4.37[b]	–	3.205	4.5[b]	–
c_0 (Å)	–	–	–	4.909	–	–	5.220	–	–
u	–	–	–	0.380	–	–	0.375	–	–
$^{*}B_0$	389.7	369[a]	–	203	–	–	176	–	–
$^{**}B_0$	381.2	–	–	202.9	–	–	176.3	–	–
$^{*}B'$	3.3	4[a]	–	3.7	–	–	4.37	–	–
$^{**}B'$	3.6	–	–	3.86	–	–	4.10	–	–
C_{11}	812	–	818.9[e]	407.6	–	376[f]	334.6	264[d]	
C_{12}	162.9	–	188.7[e]	128.8	–	121[f]	113	153[d]	
C_{13}	–	–	–	93.46	–	93[f]	76.3	–	–
C_{33}	–	–	–	386.8	–	351[f]	385.7	–	–
C_{44}	462.9	–	–	128.4	–	115[f]	93.75	68[d]	
G	401	–	460.2[e]	137.8	–	–	110.4	–	–
B/G	0.97	–	–	1.471	–	–	1.597	–	–
B/C_{44}	0.84	–	–	1.58	–	–	1.87	–	–
E	890.4	–	–	337.3	–	–	274.1	–	–
σ	0.11	–	–	0.22	–	–	0.24	–	–

[a]Knittle *et al* [13].
[b]Van Vechten *et al* [14].
[c]Rodriguez-Hernandez *et al* [15].
[d]Sherwin and Drummond [16].
[e]Saib and Bouarissa [17].
[f]Saib and Bouarissa [18].

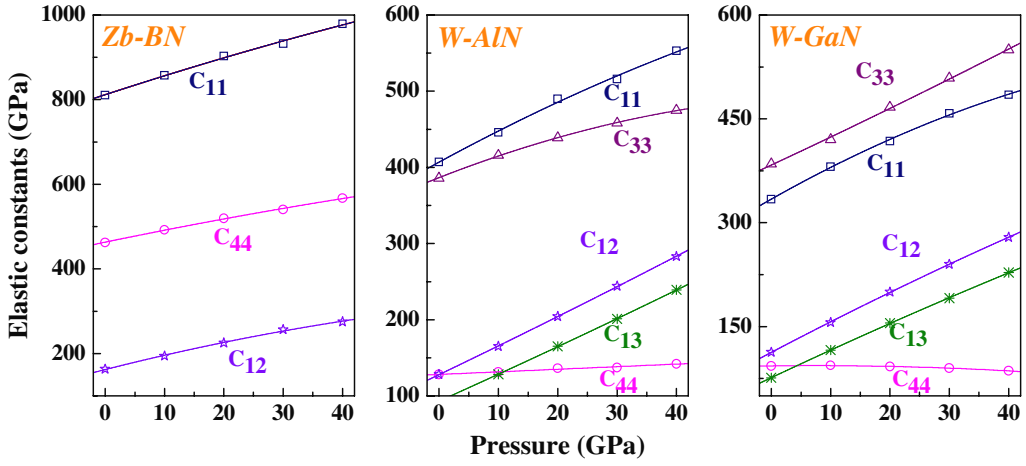

Figure 2. Elastic constants of the zinc-blende BN and wurtzite lattice AlN and GaN as a function of pressure.

the anisotropy factor $A = 2C_{44}/(C_{11} - C_{12})$. For an isotropic crystal, A is equal to 1, while any value smaller or larger than 1 indicates anisotropy. The magnitude of the deviation from 1 is a measure of the degree of elastic anisotropy possessed by the crystal. We find that $A = 0.34$, 0.66 and 0.84 for BN, AlN and GaN, and as a result, the anisotropy is strong when going from BN to GaN.

From the theoretical elastic constants, we computed the elastic wave velocities. The single-crystal elastic wave velocities in different directions are given by the resolution of the Cristoffel equation [22]:

$$(C_{ijkl}n_j n_k - \rho v^2 \delta_{il})u_l = 0, \quad (1)$$

where C_{ijkl}, n, ρ, u and v are the single-crystal elastic constant tensor, the wave propagation direction, the density of material, the wave polarization and the wave velocity, respectively. The solutions of this equation are of two types: a longitudinal wave with polarization parallel to the direction of propagation (v_l) and two shear waves (v_{t1} and v_{t2}) with polarization perpendicular to n. At zero pressure, for the wurtzite lattice AlN (GaN), the longitudinal wave 8026 ms^{-1} (10926 ms^{-1}) is fastest along [001] ([100]), while the shear wave 3957 ms^{-1} (6132 ms^{-1}) is slowest along [001] ([001]). In contrast, the zinc blende BN shows the fastest longitudinal wave 16720 ms^{-1} along [111] and the slowest value was 9543 ms^{-1} along [110].

Once the elastic constants are determined, the isotropic bulk modulus B and shear modulus G are determined [23]. These quantities cannot, in general, be calculated directly from the C_{ij}, but we can use our computed values to place bounds on the isotropic moduli. Reuss and Angew [24]

found lower bounds for all lattices, while Voigt discovered upper bounds [25]. Hill [26] has shown that the Voigt and Reuss averages are limits and suggested that the actual effective moduli could be approximated by the arithmetic mean of the two bounds. The formulae of these bounds for the hexagonal lattice can been found in [23]. We also calculated Young's modulus E and Poisson's ratio σ, which are frequently measured for polycrystalline materials when investigating their hardness. These quantities are related to the bulk modulus B and the shear modulus G by the following equations [27]:

$$E = \frac{9BG}{3B+G}, \qquad \sigma = \frac{3B-E}{6B}. \tag{2}$$

The calculated Young's modulus E and Poisson's ratio σ of wurtzite AlN and GaN and the zinc blende BN are given in table 1. Young's modulus is a measure of the stiffness of a given material, whereas Poisson's ratio is the ratio (when a sample is stretched) of the contraction or transverse strain to the extension or axial strain. The values of σ obtained for the materials of interest range between -1 and 0.5. From E and σ values, we note that GaN has a lower stiffness and a greater lateral expansion compared with AlN and BN, respectively.

3.3. Calculation of the Debye temperature

Having calculated Young's modulus E, bulk modulus B and shear modulus G, one can calculate the Debye temperature, which is an important fundamental parameter closely related to many physical properties such as elastic constants, specific heat and melting temperature. At low temperature, the vibrational excitation arises solely from acoustic mode. Hence, at low temperature, the Debye temperature calculated from elastic constants is the same as that determined from specific heat measurements. One of the standard methods to calculate the Debye temperature (θ_D) is from elastic data, since θ_D may be estimated from the average sound velocity v_m by the following equation [28]:

$$\theta_D = \frac{h}{k_B}\left[\frac{3}{4\pi V_a}\right]^{1/3} v_m \tag{3}$$

where h, k_B and V_a are Planck's constant, Boltzmann's constant and atomic volume, respectively. The average sound velocity of the polycrystalline material is given by [27]

$$v_m = \left[\frac{1}{3}\left(\frac{2}{v_t^3}+\frac{1}{v_l^3}\right)\right]^{-1/3} \tag{4}$$

where v_l and v_t are the longitudinal and transverse sound velocities of an isotropic aggregate obtained using the shear modulus G and the bulk modulus B from Navier's equation [27]:

$$v_l = \left(\frac{3B+4G}{3\rho}\right)^{1/2} \quad \text{and} \quad v_t = \left(\frac{G}{\rho}\right)^{1/2}. \tag{5}$$

The values of density 3.41 (5.98) and 3.54, longitudinal wave 10645 (7109) and 16141, transverse wave 4809 (4412) and 8235, and average sound velocity 5423 (4864) and 9227 m s^{-1} calculated by using equations (4) and (5) are for wurtzite AlN (GaN) and zinc-blende BN at zero pressure. No experimental or theoretical data about these parameters are available that could be compared with our prediction results. We illustrate in figure 3 the dependence of the Debye temperature (θ_D) on pressure for the zinc-blende BN and the wurtzite AlN and GaN. It increases monotonically when the pressure is enhanced for all these binary compounds. At zero pressure, the Debye temperature values reported in this work for wurtzite AlN and zinc-blende BN are in good agreement with those reported by Peng *et al* (1089 K) [30] and Inaba and Yoshiasa (1850 K) [29], respectively.

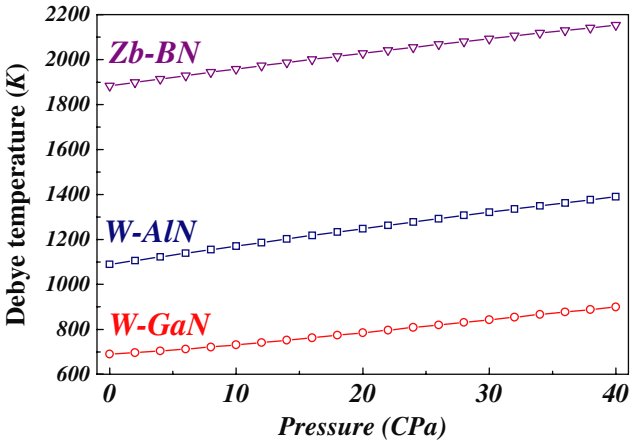

Figure 3. Dependence of the Debye temperature on pressure for wurtzite structures AlN and GaN and zinc-blende BN.

3.4. Electronic properties

In figure 4, we show the electronic band dispersion curves along some high-symmetry directions of the Brillouin zone calculated for the equilibrium geometry of wurtzite AlN and GaN and zinc-blende BN within GGA. The results show that at zero pressure, both AlN and GaN materials are direct Γ–Γ band-gap semiconductors, while BN has an indirect band gap Γ–X. The main band gap values at equilibrium Γ–Γ for wurtzite GaN and AlN and at Γ–X for zinc-blende BN at zero pressure, along with other calculations, are 1.96 (1.886) eV [31], 4.81 (4.73) eV [32] and 4.65 (4.45) [33] eV, respectively. The equilibrium value of Γ–K for AlN was 5.58 eV. The effect of pressure on the size of the energy gaps at selected symmetry points was investigated. The plots of the main fundamental band gaps versus pressure within the GGA approach are shown in figure 5. All the calculated band gaps are well fitted to a quadratic function:

$$\begin{aligned} E_{BN}^{\Gamma-X}(P) &= 4.654 + 0.002P + 4.25x10^{-7}P^2, \\ E_{GaN}^{\Gamma-\Gamma}(P) &= 1.97 + 0.035P - 2.23x10^{-4}P^2, \\ E_{AlN}^{\Gamma-\Gamma}(P) &= 4.821 + 0.041P - 2.22x10^{-5}P^2, \\ E_{AlN}^{\Gamma-K} &= 5.585 + 0.015P - 8.57x10^{-5}P^2. \end{aligned} \tag{6}$$

One can see that all fundamental band gaps increase with increasing pressure. The direct Γ–Γ band gap in AlN becomes an indirect Γ–K band gap at about 35 GPa.

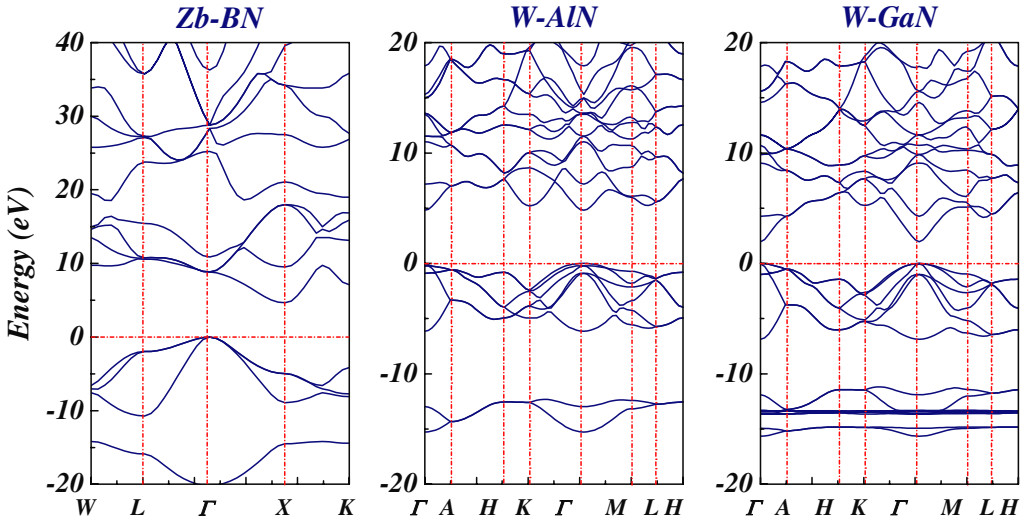

Figure 4. Band structures of the binary zinc-blende BN and wurtzite phases GaN and AlN. The Fermi level is located at 0 eV.

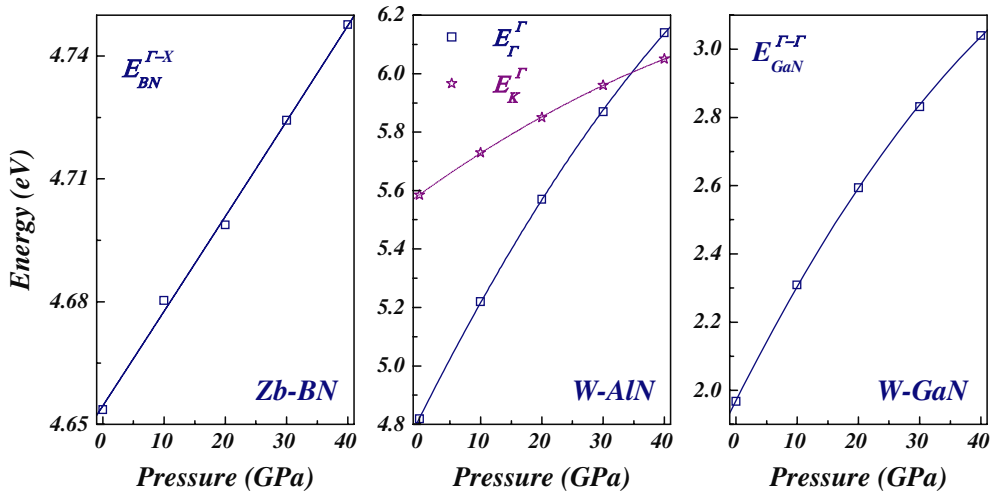

Figure 5. Plots of the main fundamental band gaps of zinc-blende BN and wurtzite phases AlN and GaN versus pressure.

The partial and total density of phonon states (PDOS and TDOS) of wurtzite AlN and GaN and zinc-blende BN within the energy interval from (E_F–10 eV) up to (E_F + 20 eV) are reported in figure 6. The top of the valence band consists of N–p states mixed with B–p, Al–p and Ga–p states and there is hybridization between the N–p state and B–p, Al–p and Ga–p states in the top of the valence band for all structures. The N–p states contribute preferably to the top of the valence band. The top of the valence bands reflects *p* electronic character for all structures. Above the Fermi level, the conduction band (CB) is dominated by B–p, Ga–p mixed with Ga–s and Al–p states, and it is more dispersive than the valence band.

3.5. Lattice dynamic and dielectric properties

We treat the lattice vibration in terms of the vibration norm-modes for each type of the phonon frequency (acoustical or optical) and also the wave propagation type (longitudinal or transversal). The creation of the phonons and their diffusion in the lattice are due to the temperature effects. The calculated phonon dispersion curves for the wurtzite AlN and GaN and zinc-blende BN along several high-symmetry

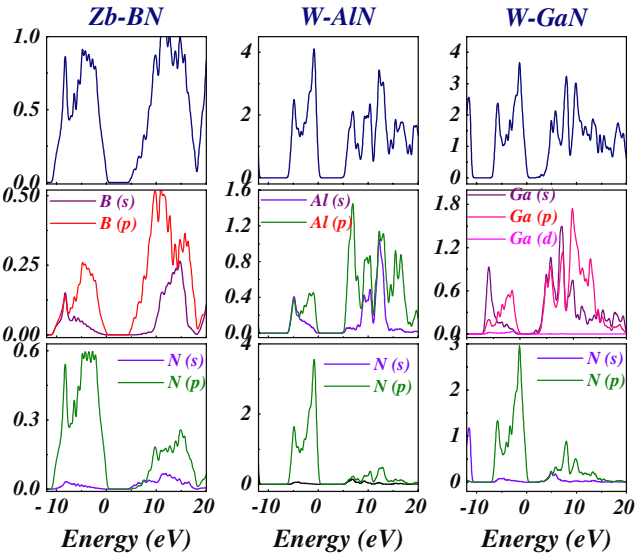

Figure 6. Calculated PDOS and TDOS of the binary zinc-blende BN and wurtzite phases AlN and GaN.

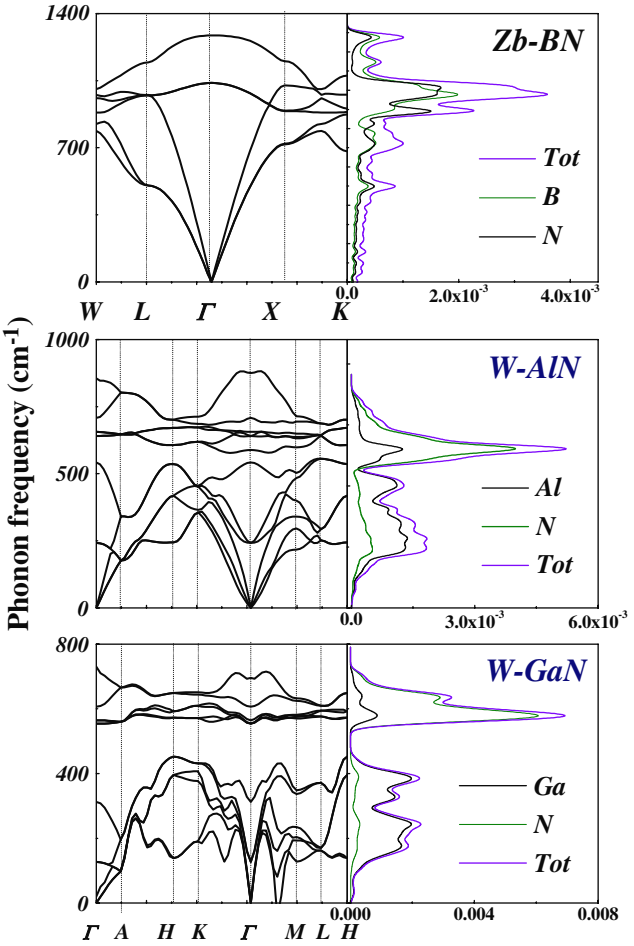

Figure 7. Calculated phonon dispersion curves and PDOS of zinc-blende BN and wurtzite phases AlN and GaN.

Table 2. Phonon frequencies in units of cm^{-1} for the zinc-blende BN and wurtzite AlN and GaN at zero pressure.

	Mode	Zb-BN	W-AlN		W-GaN	
			TW	Other	TW	Other
Γ	E_1(LO)		875.2	915[b]	748.2	752.2[a]
Γ	A_1(LO)		807.6	890[b]	745	751.2[a]
Γ	E_{2high}		640.7	657[b]	558.8	581[a]
Γ	A_1(TO)		588.6	610[b]	553.9	545.2[a]
Γ	E_{2low}		252.1		126.7	144[a]
Γ	E_1(TO)		542.3		353.9	
Γ	LO(Zb)	1280.5				
Γ	TO(Zb)	1059.3				
A	LO		802.3		665.4	735.2[a]
A	LA		176.2		196.2	239.4[a]
M	A_1(TO)		598.4		575.7	601.6[a]
M	E_2		399.7		234.9	240.7[a]
M	E_2		342.1	248[b]	203.6	199.6[a]
M	TA_z		295.5		193.6	140.5[a]
M	Ta_2		217.3		128.9	
K	A_1TO		619.4		571.5	
K	TA like		356.		190.7	215.5[b]

[a]Ruf *et al* [34].
[b]Dingle *et al* [38].

lines, with the TDOS and PDOS are shown in figure 7. The resulting phonon frequencies for the high-symmetry points in the wurtzite GaN and AlN and zinc-blende BN are listed in table 2. The frequencies of some high-symmetry

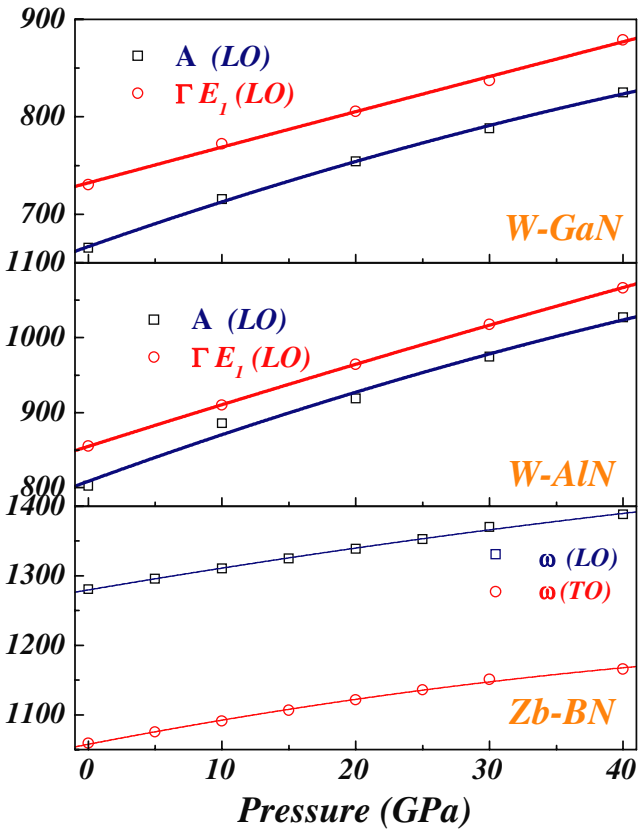

Figure 8. Pressure dependence of the ω_{LO} and ω_{TO} of zinc-blende BN, Γ (E_2(LO)) and A (LO) for wurtzite AlN and GaN.

phonons in wurtzite-type GaN of this work are in reasonable agreement with those reported in [34]. Our longitudinal and transversal optical phonon frequencies, ω_{L0} and ω_{T0}, for zinc-blende BN are in good agreement with experiment data, 1305 and 1055 cm^{-1} [35], and theoretical data, 1285 cm^{-1} [36] and 1054.7 cm^{-1} [32]. Our frequencies for the LO and TO modes at zero pressure in wurtzite AlN are in reasonable agreement with those reported by Sanjurjo *et al* [37] (893 and 667.5 cm^{-1}) and Dingle *et al* [38]. The main features shown by the phonon dispersion spectra of lead nitride compounds are the following.

1. The shapes of the phonon dispersion spectra of GaN, AlN and BN are similar.
2. The LO and TO branches are separated by a small gap for AlN and GaN, whereas they overlap in BN.
3. All phonon frequencies are positive and this indicates that AlN, GaN and BN are stable throughout the Brillouin zone.
4. There is a gap between optical and acoustic modes in AlN and GaN, whereas these modes overlap in BN. The PDOSs of all compounds show a continuous density of phonon states. The observed gap for GaN is greater than that for AlN.

The variation of phonon frequencies at A and Γ points for the LO and E_1LO modes in wurtzite AlN and GaN and the longitudinal and transversal phonon frequencies for zinc blende BN as a function of pressure is illustrated in figure 8. These modes show a nearly linearly increase when the pressure is enhanced.

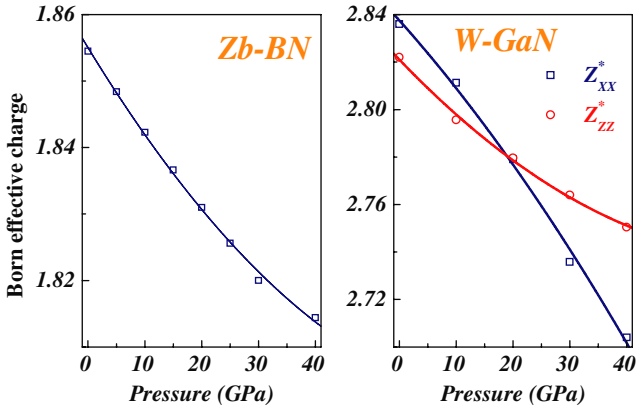

Figure 9. BEC versus pressure for zinc-blende BN and wurtzite GaN.

The Born effective charge (BEC) tensor $Z(k)_{ij}$ can be defined either as a force in direction i on atom k that results from a unitary electric field applied along direction j or as the polarization induced in direction i due to the unitary displacement in direction j of all atoms k. The full tensors of the BEC for the constituents of zinc-blende BN and wurtsite phase AlN and GaN can be written as follows:

$$Z_{\mathrm{N}}^{\mathrm{BN}} = \begin{bmatrix} -1.856 & 0 & 0 \\ 0 & -1.856 & 0 \\ 0 & 0 & -1.856 \end{bmatrix},$$

$$Z_{\mathrm{B}}^{\mathrm{BN}} = \begin{bmatrix} 1.854 & 0 & 0 \\ 0 & 1.854 & 0 \\ 0 & 0 & 1.854 \end{bmatrix},$$

$$Z_{\mathrm{N}}^{\mathrm{AlN}} = \begin{bmatrix} -2.459 & 0 & 0 \\ 0 & -2.459 & 0 \\ 0 & 0 & -2.632 \end{bmatrix},$$

$$Z_{\mathrm{Al}}^{\mathrm{AlN}} = \begin{bmatrix} 2.459 & 0 & 0 \\ 0 & 2.459 & 0 \\ 0 & 0 & 2.632 \end{bmatrix},$$

$$Z_{\mathrm{N}}^{\mathrm{GaN}} = \begin{bmatrix} -2.836 & 0 & 0 \\ 0 & -2.836 & 0 \\ 0 & 0 & -2.822 \end{bmatrix},$$

$$Z_{\mathrm{Ga}}^{\mathrm{GaN}} = \begin{bmatrix} 2.836 & 0 & 0 \\ 0 & 2.836 & 0 \\ 0 & 0 & 2.822 \end{bmatrix}. \quad (7)$$

The diagonal components at B, Al and Ga sites are equal and the off-diagonal components are negligible. The BEC analysis accordingly reconfirms that the B, Al, Ga (N) sites of BN, AlN and GaN series give up (gain) nearly 2, 2, 3 (3) electrons, respectively. The variation of the diagonal components Z_{xx}, Z_{yy} and Z_{zz} for zinc-blende BN and wurtsite GaN versus pressure is illustrated in figure 9. The BEC decreases monotonically with increasing pressure. The

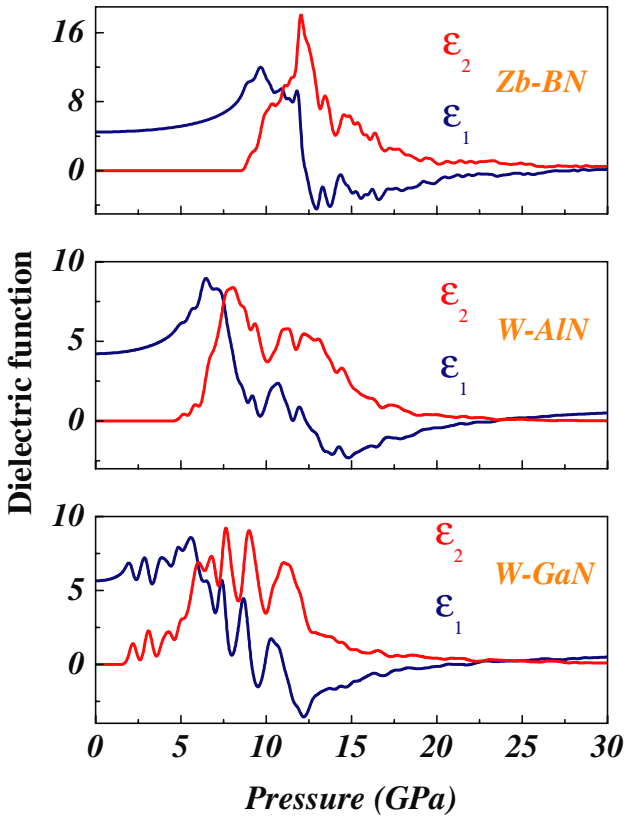

Figure 10. Real and imaginary parts of the dielectric function as a function of photon energy for zinc-blende BN and wurtzite AlN and GaN.

pressure dependence of the BEC was fitted by a quadratic polynomial fit giving the following relations:

$$Z^*_{\mathrm{BN}}(P) = 1.854 - 0.001P + 3.9x10^{-6}P^2,$$
$$Z^{\mathrm{GaN}}_{xx}(P) = 2.8375 - 0.0026P - 1.79x10^{-5}P^2, \quad (8)$$
$$E^{\mathrm{GaN}}_{zz}(P) = 2.821 - 0.00249P + 1.87x10^{-5}P^2.$$

3.6. Optical properties

The study of compounds with cubic symmetry requires the calculation of only one dielectric tensor component for characterizing of the linear optical properties. The imaginary part of the dielectric function $\varepsilon_2(\omega)$ was calculated using the expression given in [39]. The real part $\varepsilon_1(\omega)$ of the dielectric function can be derived from the imaginary part using the Kramers–Kronig relation. From the real and imaginary parts of the dielectric function, one can calculate the refractive index using the expressions given in [40]. We show the real and imaginary parts of the dielectric function as a function of photon energy for zinc-blende BN and wurtzite AlN and GaN in figure 10. The threshold energy of the dielectric function occurs at 8.37, 4.8 and 1.81 eV for BN, AlN and GaN, respectively. The main peaks in the spectra are located at 12.02, 8.05 and 7.6 eV for BN, AlN and GaN, respectively, and they correspond to the transition from the occupied N–p (valence band) states to the unoccupied B–p, Al–p and Ga–p (conduction band) states. For the interpretation of the optical spectra, it seems

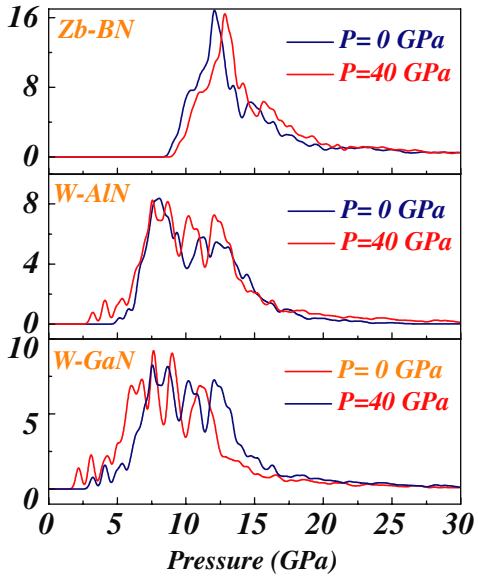

Figure 11. Effect of pressure on the imaginary part of the dielectric function for zinc-blende BN and wurtzite AlN and GaN.

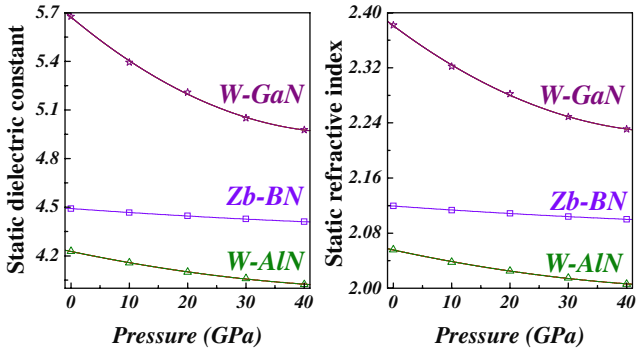

Figure 12. The static dielectric constant and static refractive index of zinc-blende BN and wurtzite AlN and GaN as a function of pressure.

unrealistic to attribute the transitions only to the present peaks in spectra, because many transitions can be observed in the band structure with an energy corresponding to the same peak. Figure 11 shows that when these compounds are compressed, the threshold energies and the main peaks were shifted toward higher energies for the wurtzite AlN and GaN and toward lower energies in zinc-blende BN. Under pressure, the shape of the profile is similar to that at equilibrium. Figure 12 shows the variation of the static dielectric constant and static refractive index for the wurtzite AlN and GaN and zinc-blende BN as a function of pressure. The static dielectric constant $\varepsilon_1(0)$ is found to be 4.49, 4.22 and 5.67 for BN, AlN and GaN, respectively. The static refractive index is found to have the values 2.11, 2.05 and 2.38 for BN, AlN and GaN, respectively. We note that these parameters decrease monotonically with increasing pressure. The static dielectric constant and static refractive index are indeed inversely proportional to the fundamental band gap of all compounds. The decrease of ε and n in BN compounds is weaker, and this can be explained by their higher elastic constants. The pressure dependence of the static dielectric constant and static refractive index was fitted by a quadratic polynomial fit giving the following relations:

$$\begin{aligned}
\varepsilon_1^{\mathrm{BN}} &= 4.464 - 0.002 \times P + 4 \times 10^{-5} P^2, \\
n^{\mathrm{BN}} &= 2.112 - 5.36 \times 10^{-4} \times P + 1.35 \times 10^{-6} P^2, \\
\varepsilon_1^{\mathrm{AlN}} &= 4.227 - 0.007 \times P + 6.21 \times 10^{-5} P^2, \\
n^{\mathrm{AlN}} &= 2.055 - 1.8 \times 10^{-3} \times P + 1.5 \times 10^{-5} P^2, \\
\varepsilon_1^{\mathrm{GaN}} &= 5.673 - 0.03 \times P + 3.18 \times 10^{-4} P^2, \\
n^{\mathrm{GaN}} &= 2.381 - 6.30 \times 10^{-3} \times P + 6.5 \times 10^{-5} P^2.
\end{aligned} \tag{9}$$

4. Conclusion

We have presented a study of the structural, elastic, electronic, phonon frequency and optical properties of zinc-blende BN and wurtzite phases AlN and GaN employing the pseudo-potential plane wave approach. The hydrostatic pressure affects strongly all elastic constants, except for C_{44} in wurtzite AlN and GaN. AlN and GaN present a direct band gap Γ–Γ, whereas BN has an indirect band gap Γ–X. The indirect Γ–K band gap in AlN occurs at about 35 GPa. The BEC of the constituents of zinc-blende BN and wurtzite phases AlN and GaN can be written as a tensor with equal diagonal components at B, Al and Ga sites. All phonon frequencies are positive throughout the Brillouin zone and this indicates that these compounds are stable.

References

[1] Ponce F A and Bour D P 1997 *Nature* **386** 351
[2] Nakamura S and Fasol G 1997 *The Blue Laser Diode* (Berlin: Springer)
[3] Nakamura S 1999 *Semicond. Sci. Technol.* **14** R27
Nakamura S 1999 *J. Cryst. Growth* **202** 290
[4] Sharma U S, Bisht P S and Verma U P 2009 *J. Phys.: Condens. Matter* **21** 025501
[5] Badding J V 1998 *Annu. Rev. Mater. Sci.* **28** 631
[6] Vurgaftman I and Meyer J R 2003 *J. Appl. Phys.* **94** 3675
[7] Thompson M P, Auner G W, Zheleva T S, Jones K A, Simko S J and Hilfiker J N 2001 *J. Appl. Phys.* **89** 3331
[8] Saib S and Bouarissa N 2006 *Comput. Mater. Sci.* **37** 613
[9] Segall M D, Lindan P J D, Probert M J, Pickard C J, Hasnip P J, Clark S J and Payne M C 2002 *J. Phys.: Condens. Matter* **14** 2717
[10] Hohenberg P and Kohn W 1964 *Phys. Rev.* B **136** 864
[11] Vanderbilt D 1990 *Phys. Rev.* B **41** 7892
[12] Perdew J P, Burke K and Ernzerhof M 1996 *Phys. Rev. Lett.* **77** 3865
[13] Knittle R M, Wentzcovitch R, Jeanloz and Cohen M L 1989 *Nature* **337** 349
[14] Van Vechten J A 1969 *Phys. Rev.* **182** 891
Van Vechten J A 1969 *Phys. Rev.* **187** 1007
Van Vechten J A 1973 *Phys. Rev.* B **7** 1479
[15] Rodriguez-Hernandez P, Gonzalez-Diaz M and Munoz A 1995 *Phys. Rev.* B **51** 14705
[16] Sherwin M E and Drummond T J 1991 *J. Appl. Phys.* **69** 8423
[17] Saib S and Bouarissa N 2008 *J. Alloys Compounds* **448** 11
[18] Saib S and Bouarissa N 2006 *J. Phys. Chem. Solids* **67** 1888
[19] Lepkowski S P, Majewski J A and Jurczak G 2005 *Phys. Rev.* B **72** 245201
[20] Pugh S F 1954 *Phil. Mag.* **45** 823
[21] Sun Z, Music D, Ahuja R, Li S and Schneider J M 2005 *Phys. Rev.* B **71** 193402
[22] Karki B B, Stixrude L, Clark S J, Warren M C, Ackland G J and Crain J 1977 *Am. Miner.* **82** 51

[23] Mehl M J, Klein B M and Papaconstantopoulos D A 1995 *Intermetallic Compounds: Principle and Practice (Principles* vol 1*)* ed J H Westbrook and R L Fleischeir (London: Wiley)
[24] Reuss A and Angew Z 1929 *Math. Mech.* **8** 55
[25] Voigt W 1928 *Lehrbush der Kristallphysik* (Leipzig: Teubner)
[26] Hill R 1952 *Proc. Phys. Soc.* A **65** 349
[27] Schreiber E, Anderson O L and Soga N 1972 *Elastic Constants and Their Measurements* (New York: McGraw-Hill)
[28] Anderson O L 1963 *J. Phys. Chem. Solids* **24** 909
[29] Inaba A and Yoshiasa A 1997 *Japan. J. Appl. Phys.* **36** 5644
[30] Peng F, Chen D, Fu H and Cheng X 2008 *Physica* B **403** 4259
[31] Arbouche O, Belgoumène B, Soudini B and Driz M 2009 *Comput. Mater. Sci.* **47** 432
[32] Christensen N E and Gorczyca I 1994 *Phys. Rev.* B **50** 4397
[33] Zaoui A and El-Haj Hassan F 2001 *J. Phys.: Condens. Matter* **13** 253
[34] Ruf T, Serrano J, Cardona M, Pavone P, Pabst M, Krisch M, D'Astuto M, Suski T, Grzegory I and Leszczynski M 2001 *Phys. Rev. Lett.* **86** 906
[35] Reich S *et al* 2005 *Phys. Rev.* B **71** 205201
[36] Ferhat M *et al* 1998 *J. Phys.: Condens. Matter* **10** 7995
[37] Sanjurjo J A, Lopez-Cruz E, Vogl P and Cardona M 1983 *Phys. Rev.* B **28** 4579
[38] Dingle R, Sell D D, Stokowski S E and Ilegems M 1991 *Phys. Rev.* B **44** 9056
[39] Lu L Y, Cheng Y, Chen X R and Zhu J 2005 *Physica* B **370** 236
[40] Chang J, Chen X R, Zhang W and Zhu J 2008 *Chin. Phys.* B **17** 1377